# Effect of atomic vibrations on the x-ray absorption spectra at the *K* edge of Al in $\alpha$-$Al_2O_3$ and of Ti in $TiO_2$ rutile

Christian Brouder, Delphine Cabaret, Amélie Juhin, and Philippe Sainctavit
*Institut de Minéralogie et de Physique des Milieux Condensés, CNRS UMR 7590, IPGP, Université Pierre et Marie Curie-Paris 6–Université Denis Diderot-Paris 7, 140 rue de Lourmel, 75015 Paris, France*

(Received 2 December 2009; revised manuscript received 15 February 2010; published 17 March 2010)

The influence of atomic vibrations on x-ray absorption near-edge structure is calculated by assuming that vibrational energies are small with respect to the instrumental resolution. The resulting expression shows that, at the *K* edge, vibrations enable electric-dipole transitions to 3*s* and 3*d* final states. The theory is applied to the *K* edge of Al in $\alpha$-$Al_2O_3$ and of Ti in $TiO_2$ rutile and compared with experiment. At the Al *K* edge, sizeable transitions toward 3*s* final states are obtained, leading to a clear improvement of the agreement with experimental spectra. At the Ti *K* edge, electric-dipole transitions toward 3*d* final states explain the temperature dependence of the pre-edge features.

DOI: 10.1103/PhysRevB.81.115125 PACS number(s): 78.70.Dm, 65.40.−b

## I. INTRODUCTION

Vibronic coupling describes the interaction between electrons and nuclear motions. It plays a prominent role in optical spectroscopy where it is the source of the color of many pigments and gemstones.[1] For instance, the red color of Black Prince's ruby is due to "*d-d*" transitions of chromium impurities in a spinel crystal. However, these transitions are forbidden because chromium occupies an inversion center of the spinel lattice. They become allowed when vibrations break inversion symmetry.

In the x-ray range, vibrations far from the edge are taken into account[2] through a Debye-Waller factor $e^{-2k^2\sigma^2}$. If the validity of this factor is assumed to extend to the near-edge region, where $k \simeq 0$, then vibrations seem negligible in x-ray absorption near-edge structure (XANES) spectra.

However, three arguments indicate that vibronic coupling can be sizeable in the XANES region: (i) vibronic coupling was detected by x-ray resonant scattering experiments at the Ge *K* edge;[3,4] (ii) some XANES peaks seem to be due to forbidden transitions to 3*s* states, a prominent example being the Al *K* edge in minerals;[5] and (iii) a temperature dependence of the pre-edge structure was observed at the Ti *K* edge of several titanium oxides.[6,7]

In the optical range, the effect of vibrations is usually taken into account through the Franck-Condon factors. In the x-ray range, Fujikawa and co-workers showed in a series of papers of increasing sophistication[8–10] that the effect of the Franck-Condon factors can be represented by the convolution of the "phononless" x-ray absorption spectrum with the phonon spectral function. Such a convolution leads to a broadening of the peaks with increasing temperature but this effect is hardly observable in the pre-edge region.

Besides, Mäder and Baroni[11] showed that the large core-electron-phonon coupling of the 1*s* core hole of carbon in diamond induces a strong lattice distortion and significant anharmonic contributions in the final state of the x-ray absorption process.

The key observation is that all these effects can be easily taken into account if the vibrational energies are small with respect to the XANES spectral resolution (core hole lifetime+instrumental resolution). This condition is not satisfied at the C *K* edge[11] but it becomes reasonable at the Al and Ti *K* edges. In that range the XANES resolution is around 1 eV whereas the energy of vibrational modes is on the order of a few hundredths of electron volt although, of course, several phonons can be simultaneously present.

In this paper, we first use this observation to derive a manageable expression for the vibronically coupled x-ray absorption spectra. Then, we apply the so-called *crude Born-Oppenheimer* approximation to further simplify this expression, so that only the core-hole motion remains. The resulting equation is compared with experiment in two different cases. At the Al *K* edge in $\alpha$-$Al_2O_3$ (corundum), vibrations induce transitions to 3*s* final states. These $1s \to 3s$ dipole transitions explain a pre-edge peak that is completely absent from standard calculations. At the Ti *K* edge in $TiO_2$ (rutile), $1s \to 3d$ transitions are induced by vibrations. This explains why only the first two pre-edge peaks grow with temperature.

## II. BORN-OPPENHEIMER APPROXIMATION

For a system of $N$ nuclei and $M$ electrons with position vectors $\mathbf{Q}_1, \ldots, \mathbf{Q}_N$ and $\mathbf{r}_1, \ldots, \mathbf{r}_M$, respectively, we define the collective coordinates $\mathbf{Q}=(\mathbf{Q}_1, \ldots, \mathbf{Q}_N)$ and $\bar{\mathbf{r}}=(\mathbf{r}_1, \ldots, \mathbf{r}_M)$. The wave function $\Psi(\bar{\mathbf{r}}, \mathbf{Q})$ of the system is the solution of the Schrödinger equation

$$(H_{ee} + V_{en} + V_{nn} + H_{kin})\Psi(\bar{\mathbf{r}}, \bar{\mathbf{Q}}) = E\Psi(\bar{\mathbf{r}}, \bar{\mathbf{Q}}), \qquad (1)$$

where $H_{ee}=H_{ee}(\bar{\mathbf{r}})$ is the Hamiltonian taking into account the electron kinetic energy and the electron-electron interaction (and possibly the spin-orbit interaction), $V_{en}=V_{en}(\bar{\mathbf{r}}, \bar{\mathbf{Q}})$ is the Coulomb potential between electrons and nuclei, $V_{nn}=V_{nn}(\bar{\mathbf{Q}})$ is the Coulomb potential between nuclei, and $H_{kin}=H_{kin}(\bar{\mathbf{Q}})$ is the nuclear kinetic energy. According to the Born-Oppenheimer approximation,[12,13] $\Psi(\bar{\mathbf{r}}, \bar{\mathbf{Q}})$ can be approximated by the product $\chi_n^j(\bar{\mathbf{Q}})\psi_n(\bar{\mathbf{r}}; \bar{\mathbf{Q}})$, where the electronic wave function $\psi_n(\bar{\mathbf{r}}; \bar{\mathbf{Q}})$ is the solution of

 

$$(H_{ee} + V_{en} + V_{nn})\psi_n(\bar{\mathbf{r}};\bar{\mathbf{Q}}) = \epsilon_n(\bar{\mathbf{Q}})\psi_n(\bar{\mathbf{r}};\bar{\mathbf{Q}}), \tag{2}$$

and describes the state of the electrons in a potential where the nuclei are fixed at position $\bar{\mathbf{Q}}$. The ground state corresponds to $n=0$. The origin of the nuclear variables is chosen so that $\bar{\mathbf{Q}}=\bar{\mathbf{0}}$ is the equilibrium position, i.e., $\epsilon_0(\bar{\mathbf{0}})$ is the minimum of $\epsilon_0(\bar{\mathbf{Q}})$.

For each $n$, the vibrational wave functions $\chi_n^j(\bar{\mathbf{Q}})$ are the orthonormal solutions of the Schrödinger equation

$$[H_{kin}(\bar{\mathbf{Q}}) + \epsilon_n(\bar{\mathbf{Q}})]\chi_n^j(\bar{\mathbf{Q}}) = E_n^j\chi_n^j(\bar{\mathbf{Q}}), \tag{3}$$

where $E_n^j$ is the total energy of the electrons+nuclei system. Within the Born-Oppenheimer approximation, the x-ray absorption cross-section is

$$\sigma(\omega) = 4\pi^2\alpha_0\hbar\omega\sum_{fj}\left|\int d\bar{\mathbf{Q}}d\bar{\mathbf{r}}\chi_f^j(\bar{\mathbf{Q}})^*\psi_f(\bar{\mathbf{r}};\bar{\mathbf{Q}})^*\hat{\varepsilon}\cdot\bar{\mathbf{r}} \times \chi_0(\bar{\mathbf{Q}})\psi_0(\bar{\mathbf{r}};\bar{\mathbf{Q}})\right|^2\delta(E_f^j - E_0 - \hbar\omega), \tag{4}$$

where $\alpha_0$ is the fine structure constant, $\hbar\omega$ the energy of the incident x rays, $\hat{\varepsilon}$ their polarization vector, and $\hat{\varepsilon}\cdot\bar{\mathbf{r}}=\Sigma_i\hat{\varepsilon}\cdot\mathbf{r}_i$. The core-hole lifetime and the instrumental resolution can be represented by the convolution of the absorption cross-section with a Lorentzian function $(\Gamma/\pi)/(\omega^2+\Gamma^2)$. This gives us

$$\sigma_\gamma(\omega) = 4\pi\alpha_0\sum_{fj}\left|\int d\bar{\mathbf{Q}}d\bar{\mathbf{r}}\chi_f^j(\bar{\mathbf{Q}})^*\psi_f(\bar{\mathbf{r}};\bar{\mathbf{Q}})^*\hat{\varepsilon}\cdot\bar{\mathbf{r}} \times \chi_0(\bar{\mathbf{Q}})\psi_0(\bar{\mathbf{r}};\bar{\mathbf{Q}})\right|^2\frac{(E_f^j - E_0^0)\gamma}{(E_f^j - E_0 - \hbar\omega)^2 + \gamma^2}, \tag{5}$$

where $\gamma=\hbar\Gamma$.

## III. APPROXIMATIONS

Equation (5) cannot be evaluated for realistic crystals and approximations have to be made. In the first approximation, we consider that the vibrational energy is small with respect to the instrumental resolution. The second approximation deals with the core-hole wave function, which is considered to be independent of the rest of the crystal, and with the final-state wave function, which is taken in the crude Born-Oppenheimer approximation. Finally, we describe the nuclear motion in the harmonic approximation.

The energy $E_f^j$ can be written as the sum of the electronic energy at equilibrium position $\epsilon_f=\epsilon_f(\bar{\mathbf{0}})$ and a vibrational energy $E_{vib}^{fj}$. When $\gamma$ is much larger than the vibrational energy we can neglect the contribution of $E_{vib}^{fj}$ and sum over the vibrational states $\chi_f^j(\bar{\mathbf{Q}})$. The completeness relation gives us

$$\sum_j \chi_f^j(\bar{\mathbf{Q}})^*\chi_f^j(\bar{\mathbf{Q}}') = \delta(\bar{\mathbf{Q}} - \bar{\mathbf{Q}}'). \tag{6}$$

Therefore,

$$\sigma_\gamma(\omega) = 4\pi\alpha_0\int d\bar{\mathbf{Q}}\sum_f\left|\int d\bar{\mathbf{r}}\psi_f(\bar{\mathbf{r}};\bar{\mathbf{Q}})^*\hat{\varepsilon}\cdot\bar{\mathbf{r}} \times \chi_0(\bar{\mathbf{Q}})\psi_0(\bar{\mathbf{r}};\bar{\mathbf{Q}})\right|^2\frac{(\epsilon_f - \epsilon_0)\gamma}{(\epsilon_f - \epsilon_0 - \hbar\omega)^2 + \gamma^2}. \tag{7}$$

Note that we derived this result without making the harmonic approximation. Therefore, the possible anharmonic behavior due to the core hole[11] is taken into account.

Now we make a different approximation for the initial and final electronic states. For a $K$ edge, the $1s$ core-level wave function is highly localized around the nucleus and it weakly depends on the surrounding atoms. Therefore, we can approximate $\psi_0(\bar{\mathbf{r}};\bar{\mathbf{Q}})$ by $\phi_0(\mathbf{r}-\mathbf{Q}_a)$, where $\mathbf{r}$ and $\mathbf{Q}_a$ are the position vectors of the core electron and the nucleus of the absorbing atom, respectively, and where $\phi_0$ is the $1s$ wave function of the absorbing atom at equilibrium position. For the final electronic states $\psi_f(\bar{\mathbf{r}};\bar{\mathbf{Q}})$ in the presence of a core hole, the variation in the nuclear coordinates $\bar{\mathbf{Q}}$ in Eq. (7) is ruled by the vibrational wave function $\chi_0$ of the initial state, which is expected to be rather smooth. Therefore, we make the standard *crude* Born-Oppenheimer approximation, according to which the electronic wave function does not significantly vary with $\bar{\mathbf{Q}}$ for small vibrational motions. In other words, $\psi_f(\bar{\mathbf{r}};\bar{\mathbf{Q}})\simeq\psi_f(\bar{\mathbf{r}};\bar{\mathbf{0}})$. Electric-dipole transitions being represented by a one-particle operator, the transitions can be written in terms of matrix elements between one-particle orbitals. We use orbitals calculated in the Kohn-Sham implementation of the density-functional theory. Thus, the final states will be represented by one-electron wave functions $\phi_f(\mathbf{r})$. This gives us

$$\sigma_\gamma(\omega) = 4\pi\alpha_0\int d\bar{\mathbf{Q}}|\chi_0(\bar{\mathbf{Q}})|^2\sum_f\left|\int d\mathbf{r}\phi_f(\mathbf{r})^*\hat{\varepsilon}\cdot\mathbf{r} \times \phi_0(\mathbf{r} - \mathbf{Q}_a)\right|^2\frac{(\epsilon_f - \epsilon_0)\gamma}{(\epsilon_f - \epsilon_0 - \hbar\omega)^2 + \gamma^2}. \tag{8}$$

When the crude Born-Oppenheimer approximation is not valid, it is possible to Taylor-expand $\psi_f(\bar{\mathbf{r}};\bar{\mathbf{Q}})$ as a function of $\bar{\mathbf{Q}}$.[14] The integral over electronic variables depends only on the position of the absorbing atom, from now on denoted by $\mathbf{R}$. Therefore, we can integrate over the other nuclear variables and the expression becomes

$$\sigma_\gamma(\omega) = 4\pi\alpha_0\int d\mathbf{R}\rho(\mathbf{R})\sum_f\left|\int d\mathbf{r}\phi_f(\mathbf{r})^*\hat{\varepsilon}\cdot\mathbf{r} \times \phi_0(\mathbf{r} - \mathbf{R})\right|^2\frac{(\epsilon_f - \epsilon_0)\gamma}{(\epsilon_f - \epsilon_0 - \hbar\omega)^2 + \gamma^2}, \tag{9}$$

where $\rho(\mathbf{R})=\int d\bar{\mathbf{Q}}|\chi_0(\bar{\mathbf{Q}})|^2\delta(\mathbf{Q}_a-\mathbf{R})$. We used a ground-state phonon wave function $\chi_0(\bar{\mathbf{Q}})$ for notational convenience. The generalization to a Boltzmann distribution of phonon states is straightforward. Within the harmonic approximation, the core displacement distribution has the form[15]

$$\rho(\mathbf{R}) = \exp\left(-\frac{\mathbf{R}\cdot U^{-1}\cdot \mathbf{R}}{2}\right), \tag{10}$$

where $U$ is the thermal parameter matrix[16] that is measured in x-ray or neutron-scattering experiments.

## IV. CALCULATION OF THE MATRIX ELEMENT

For a hydrogenoid atom, the $1s$ core-hole radial wave function is proportional to $e^{-ar}$, where $a=Z/a_0$, $Z$ is the atomic number, and $a_0$ the Bohr radius. The $1s$ wave function $\phi_0(r)$ of an atom is close to that of a hydrogenoid one and can be written as a fast converging linear combination of exponentials $\phi_0(r)=\Sigma_i C_i e^{-a_i r}$. For notational convenience, we consider that the core state is described by a single term $\phi_0(r)=Ce^{-ar}$. The general case is obtained by summing over $i$ the transition amplitudes calculated for $C_i$ and $a_i$. The shifted exponential is expanded by using the Barnett-Coulson formula[17]

$$e^{-a|\mathbf{r}-\mathbf{R}|} = \sum_{n=0}^{\infty} (2n+1) P_n(\hat{\mathbf{r}}\cdot\hat{\mathbf{R}}) c_n(r,R) \tag{11}$$

with $P_n$ a Legendre polynomial and

$$c_n(r,R) = -\frac{1}{\sqrt{rR}}[r_< I'_{n+1/2}(ar_<) K_{n+1/2}(ar_>) + r_> I_{n+1/2}(ar_<) K'_{n+1/2}(ar_>)], \tag{12}$$

where $r_<$ is the smaller and $r_>$ the larger of $r$ and $R$, $I_\nu(z)$ and $K_\nu(z)$ are the modified Bessel functions, and $I'_\nu(z)$ and $K'_\nu(z)$ their derivatives with respect to $z$.

To calculate the dipole transition matrix element, we expand the final-state wave function over spherical harmonics $\phi_f(\mathbf{r})=\Sigma_{\ell m} f_{\ell m}(r) Y_\ell^m(\hat{\mathbf{r}})$. The matrix element over the electronic variable is

$$\int d\mathbf{r}\, \phi_f(\mathbf{r})^* \hat{\varepsilon}\cdot\mathbf{r}\, \phi_0(\mathbf{r}-\mathbf{R}) = \sum_{\ell m} X_\ell^m(\mathbf{R}) \tag{13}$$

with

$$X_\ell^m(\mathbf{R}) = C\sum_{n=0}^{\infty} \int d\mathbf{r} f^*_{\ell m}(r) Y_\ell^m(\hat{\mathbf{r}})^* \hat{\varepsilon}\cdot\mathbf{r}(2n+1) c_n(r,R) P_n(\hat{\mathbf{r}}\cdot\hat{\mathbf{R}}). \tag{14}$$

Standard angular-momentum recoupling techniques[18] lead to

$$\hat{\varepsilon}\cdot\mathbf{r} P_n(\hat{\mathbf{r}}\cdot\hat{\mathbf{R}}) = \frac{(4\pi)^2 r}{3(2n+1)} \sum_{\lambda=-1}^{1} \sum_{p=-n}^{n} (-1)^{\lambda+p} Y_1^{-\lambda}(\hat{\varepsilon}) \times Y_n^{-p}(\hat{\mathbf{R}}) \sum_k \sum_{q=-k}^{k} C^{kq}_{1\lambda np} Y_k^q(\hat{\mathbf{r}}), \tag{15}$$

where $C^{kq}_{1\lambda np}$ are Gaunt coefficients and $k$ takes the values $|n-1|$ and $n+1$ for $n>0$ and the single value $k=1$ for $n=0$. We obtain

$$X_\ell^m(\mathbf{R}) = \frac{(4\pi)^2 C}{3} \sum_{n=|\ell\pm1|} \int r^3 dr f^*_{\ell m}(r) c_n(r,R) \times \sum_\lambda (-1)^m Y_1^{-\lambda}(\hat{\varepsilon}) Y_n^{\lambda-m}(\hat{\mathbf{R}}) C^{\ell m}_{1\lambda n m-\lambda}, \tag{16}$$

where only $n=1$ is allowed if $\ell=0$. Equation (16) shows that transitions are now possible toward all values of the final-state angular momentum $\ell$. The core-hole wave function is still spherical, but with respect to a shifted centrum. Thus, with respect to the original spectrum, it is a sum over all angular momenta given by the Barnett-Coulson expansion. All final-states angular momenta are available in spite of the fact that only electric-dipole transitions are allowed. In particular, vibrations allow for dipole transitions to the $3s$ and $3d$ final states at the $K$ edge.

It could be worthwhile to stress a somewhat subtle fact. It is commonly stated that, because of thermal vibrations, the absorbing atom shifts from its symmetrical position and its $s$ (or $d$) orbitals can hybridize with its $p$ orbitals. In the optical range, this hybridization leads to a peak where $s$ (or $d$) density of states is strong.[19] In our approach, this effect does not occur at all because of the crude Born-Oppenheimer approximation, where the final-state wave function does not change when the absorbing atom moves. Therefore, the effect is entirely due to the fact that the shifted core-hole state gets some $p$ components when the origin of the reference frame is the absorbing atom equilibrium position. Or, if the origin of the reference frame is the center of the core-hole level, the effect is due to the fact that the $s$ and $d$ states get some $p$ components with respect to this shifted origin. But these $p$ components are due to a shifted point of view and not to hybridization. A spherical function $f(|\mathbf{r}-\mathbf{R}|)$ is indeed described by the single spherical harmonics $Y_0^0(\hat{r})$ only when $\mathbf{R}=\mathbf{0}$.

## V. GENERAL FEATURES OF VIBRATIONAL TRANSITIONS

The foregoing approach enables us to draw some general conclusions concerning the effect of vibrations on XAS pre-edge structure. This effect is measurable if the density of non-$p$ states of the system in the final state (i.e., in the presence of a core hole) is large and well localized near the Fermi energy (vibrational transitions toward $p$ states would be hidden by the allowed electric-dipole transitions). For example, just above the Fermi level, many aluminum or silicon compounds have a strong density of $3s$ states and many transition-metal compounds have a large density of $3d$ states. In the first case, vibrational transitions appear as (apparently monopole) $1s\rightarrow 3s$ transitions, which are completely excluded with electromagnetic transitions. In the second case, vibrational transitions superimpose upon electric quadrupole $1s\rightarrow 3d$ transitions. As a consequence, vibrations induce transitions at specific energies in the pre-edge but hardly modify the rest of the XANES spectrum.

A temperature dependence of vibrational transitions is expected if $U$ varies with temperature. This occurs between 0 K and room temperature if the sample has soft modes (i.e., low-energy phonons). Otherwise, vibrational transitions are

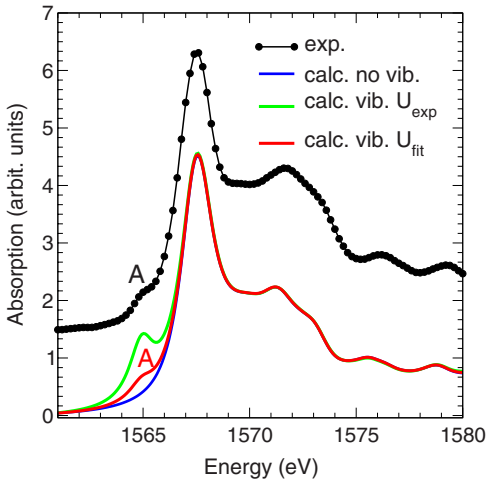


FIG. 1. (Color online) Experimental (Ref. 29) and calculated Al *K* edge isotropic spectra of corundum at 300 K. $U_{\mathrm{exp}}$ and $U_{\mathrm{fit}}$ are the experimental and fitted thermal parameters (see text).

only due to the zero-point motion of the nuclei. In other words, vibrational transitions are then a consequence of the fact that, even at 0 K, nuclei are not localized at a single point.

## VI. COMPARISON WITH EXPERIMENT

We test these conclusions with two examples: the Al *K* edge in corundum (where vibrational transitions to 3*s* states are expected) and the Ti *K* edge in rutile (where vibrational transitions to 3*d* states and a temperature dependence are expected).

The x-ray absorption cross-section within the crude Born-Oppenheimer approximation has been implemented in the XSPECTRA package[20] of the QUANTUM-ESPRESSO suite of codes.[21] To calculate the integral over **R** in Eq. (9), it is found sufficient to compute the integral over a cube of size $2\Lambda$, where $\Lambda$ is the largest eigenvalue of the matrix $U$. This cube is cut into 27 smaller cubes where the integral is carried out using Eq. (25.4.68) of Ref. 22.

We have built a $2\times2\times2$ trigonal supercell and a $2\times2\times3$ tetragonal supercell from the experimental crystallographic structure of corundum[23] and of rutile,[24] respectively. They both include a 1*s* core hole on the absorbing atom. The self-consistent charge density was determined in the generalized gradient approximation,[25] at the $\Gamma$ point of the Brillouin zone, with a 80 Ry plane-wave energy cutoff. Troullier-Martins norm-conserving pseudopotentials were used. The Ti pseudopotential was generated using the 3*s*, 3*p*, and 3*d* as valence states, the *s* states being the local part, and with 1 bohr, 1.6 bohrs, and 1.5 bohrs cut-off radii, respectively. The pseudopotentials of Al and O are defined in Ref. 26. The XANES cross-section is calculated on a $4\times4\times4$ *k*-point grid, using the method described in Ref. 27 with a broadening parameter of 0.7 eV. For additional technical details, see Refs. 26 and 28.

### A. Al *K* edge in corundum

Figure 1 compares the experimental Al *K* edge spectrum

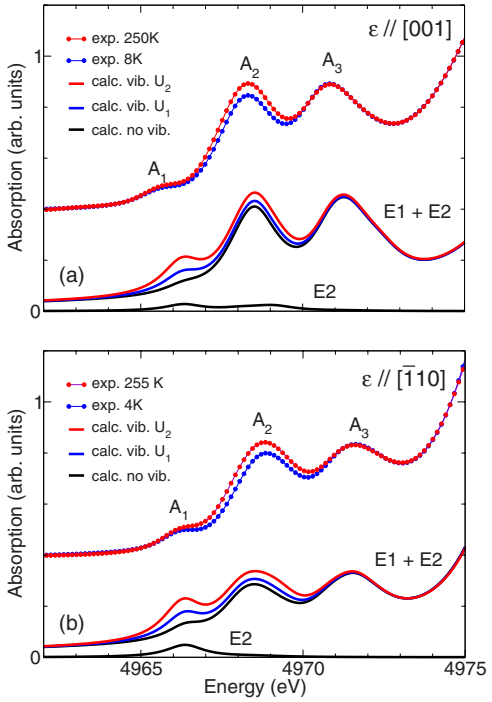


FIG. 2. (Color online) Experimental (Ref. 7) and calculated Ti *K* pre-edge spectra of rutile for polarization parallel (upper figure) and perpendicular (lower figure) to the *c* axis of the crystal. *E*1 and *E*2 are the electric-dipole and quadrupole contributions.

of corundum and the calculated ones obtained with or without taking into account the atomic vibrations. The line denoted by $U_{\mathrm{exp}}$ was obtained by using the experimental thermal parameters,[30] corresponding to the experimental mean displacements $\sigma_1=\sigma_2=0.048$ Å, $\sigma_3=0.049$ Å. The mean displacements $\sigma_i$ are the square root of the eigenvalues of $U$ and they have a more direct physical meaning than $U$. The vibration transitions are observed exactly at the position of the pre-edge peak, which is absent from the calculation without vibrations. However, the vibrational transitions are overestimated and a better agreement is obtained when setting the mean displacements to 0.026 Å (see the line denoted by $U_{\mathrm{fit}}$ in Fig. 1). Therefore, computed vibrational transitions show up at the right position but with too large an intensity. A part of this discrepancy might be due to the fact that the experimental thermal parameters include some amount of static disorder, but most of it probably comes from the crude Born-Oppenheimer approximation. The main vibrational transitions come from the *relative* displacement of the aluminum atom with respect to the six oxygen first neighbors. The vibrational modes involving an overall motion of the aluminum atom with its oxygen octahedron contribute to the thermal parameter $U$ although they only weakly contribute to the vibrational transitions. Because of the crude Born-Oppenheimer approximation, the vibrations are summarized in the thermal parameter, which overestimates the real effect of vibrations. A similar phenomenon occurs with the extended x-ray-absorption fine structure Debye-Waller factor which is different from the one determined by x-ray diffraction because only relative displacements must be taken into account. This point will be confirmed with the Ti *K* edge absorption in rutile that we consider now.

### B. Ti *K* edge of rutile

With the Ti *K* edge of rutile, we test the limit of the crude Born-Oppenheimer approximation. Indeed, this approximation assumes that the final-state wave function does not change when the crystal vibrates. This might be reasonable for the Al 3*s* states because they are poorly localized and overlap the oxygen 2*p* orbitals, but this cannot be true for the 3*d* states of Ti in rutile, which are localized near the Ti nucleus. Thus, we do not expect that the crude approximation holds at that edge.

Figure 2 shows the experimental and theoretical Ti *K* edge spectrum of rutile with the polarization parallel and perpendicular to the *c* axis and at two temperatures. The mean displacements $\sigma_1=0.0028$ Å, $\sigma_2=0.0027$ Å, and $\sigma_3=0.0023$ Å for $U_1$ and $\sigma_1=0.0043$ Å, $\sigma_2=0.0042$ Å, and $\sigma_3=0.0035$ Å for $U_2$ have been chosen to approximate the intensity of peak $A_2$ at low and room temperatures, respectively. These values are more than ten times smaller than the experimental values.[31] Moreover, when the thermal factor is adjusted to be consistent with the temperature variation in the second peak, then the temperature variation in the first peak is overestimated. This can probably be attributed to the crude Born-Oppenheimer approximation. Despite these drawbacks, several aspects of the experimental vibrational transitions are correctly reproduced: (i) only the first and the second peaks exhibit a temperature dependence, the rest of the spectrum is not modified; (ii) the peaks do not shift and do not broaden; and (iii) the peaks increase with temperature.

## VII. CONCLUSION

A model of the vibrational and temperature dependence of the near-edge features of XANES spectra was presented and compared to experiments. The theory reproduces the main aspects of the effect. In particular, it shows that the pre-edge features do not mainly originate from the hybridization due to vibrational local-symmetry breaking. This explains the observation made by Li and co-workers:[5] "it is very difficult to evaluate the correlation between the intensity of peak A and the distortion of Al coordination, even on a semiquantitative basis."

Future work will now be devoted to the measurement of the temperature dependence of other important crystals and to the elimination of the crude Born-Oppenheimer approximation.

## ACKNOWLEDGMENTS

Discussions with Christos Gougoussis and Matteo Calandra about the XSPECTRA package are gratefully acknowledged. We thank Andrei Rogalev and Vladimir Dmitrienko for useful comments. This work was performed using HPC resources from GENCI grant 2009–2015 and 1202.

[1] A. J. Bridgeman and M. Gerloch, Coord. Chem. Rev. **165**, 315 (1997).
[2] F. D. Vila, J. J. Rehr, H. H. Rossner, and H. J. Krappe, Phys. Rev. B **76**, 014301 (2007).
[3] A. Kirfel, J. Grybos, and V. E. Dmitrienko, Phys. Rev. B **66**, 165202 (2002).
[4] V. E. Dmitrienko, K. Ishida, A. Kirfel, and E. N. Ovchinnikova, Acta Crystallogr., Sect. A: Found. Crystallogr. **61**, 481 (2005).
[5] D. Li, G. M. Bancroft, M. E. Fleet, X. H. Feng, and Y. Pan, Am. Mineral. **80**, 432 (1995).
[6] S. Nozawa, T. Iwazumi, and H. Osawa, Phys. Rev. B **72**, 121101(R) (2005).
[7] O. Durmeyer, E. Beaurepaire, J.-P. Kappler, C. Brouder, and F. Baudelet, arXiv:0912.2399 (unpublished).
[8] T. Fujikawa, J. Phys. Soc. Jpn. **65**, 87 (1996).
[9] T. Fujikawa, J. Phys. Soc. Jpn. **68**, 2444 (1999).
[10] H. Arai, N. Ueno, and T. Fujikawa, *X-Ray Absorption Fine Structure–XAFS13: 13th International Conference*, AIP Conference Proceedings Vol. 882, edited by B. Hedman and P. Pianetta (AIP, New York, 2007), pp. 108–10.
[11] K. A. Mäder and S. Baroni, Phys. Rev. B **55**, 9649 (1997).
[12] M. Born and R. Oppenheimer, Ann. Phys. **389**, 457 (1927).
[13] B. Henderson and G. Imbusch, *Optical Spectroscopy of Inorganic Solids* (Clarendon, Oxford, 1989).
[14] M. Born and K. Huang, *Dynamical Theory of Crystal Lattices* (Oxford University Press, Oxford, 1954).
[15] A. A. Maradudin, E. W. Montroll, G. H. Weiss, and I. P. Ipatova, *Theory of Lattice Dynamics in the Harmonic Approximation*, Solid State Physics, 2nd ed. (Academic, New York, 1971).
[16] C. Giacovazzo, *Fundamentals of Crystallography*, 2nd ed. (Oxford University Press, Oxford, 2002).
[17] M. P. Barnett and C. A. Coulson, Philos. Trans. R. Soc. London, Ser. A **243**, 221 (1951).
[18] L. Biedenharn and J. Louck, *Angular Momentum in Quantum Physics*, Encyclopedia of Mathematics and Its Applications Vol. 8 (Addison-Wesley, Reading, 1981).
[19] C. J. Ballhausen, *Introduction to Ligand Field Theory* (McGraw-Hill, New York, 1962).
[20] C. Gougoussis, M. Calandra, A. P. Seitsonen, and F. Mauri, Phys. Rev. B **80**, 075102 (2009).
[21] P. Giannozzi *et al.*, J. Phys.: Condens. Matter **21**, 395502 (2009).
[22] M. Abramowitz and I. Stegun, *Handbook of Mathematical Functions*, 5th ed. (Dover, New York, 1964).
[23] R. E. Newnham and Y. M. de Haan, Z. Kristallogr. **117**, 235 (1962).
[24] C. J. Howard, T. M. Sabine, and F. Dickson, Acta Crystallogr., Sect. B: Struct. Sci. **47**, 462 (1991).
[25] J. P. Perdew, K. Burke, and M. Ernzerhof, Phys. Rev. Lett. **77**, 3865 (1996).
[26] D. Cabaret, E. Gaudry, M. Taillefumier, Ph. Sainctavit, and F. Mauri, Physica Scripta **T115**, 131 (2005).
[27] M. Taillefumier, D. Cabaret, A.-M. Flank, and F. Mauri, Phys. Rev. B **66**, 195107 (2002).

[28] D. Cabaret, A. Bordage, A. Juhin, M. Arfaoui, and E. Gaudry, Phys. Chem. Chem. Phys. (to be published)
[29] P. Ildefonse, D. Cabaret, Ph. Sainctavit, G. Calas, A.-M. Flank, and P. Lagarde, Phys. Chem. Miner. **25**, 112 (1998).
[30] E. N. Maslen, V. A. Streltsov, N. R. Streltsova, N. Ishizawa, and Y. Satow, Acta Crystallogr., Sect. B: Struct. Sci. **49**, 973 (1993).
[31] J. K. Burdett, T. Hughbanks, G. J. Miller, J. W. Richardson, Jr., and J. V. Smith, J. Am. Chem. Soc. **109**, 3639 (1987).